Planetary and Space Science ▮ (▮▮▮▮) ▮▮▮–▮▮▮

Contents lists available at ScienceDirect

Planetary and Space Science

journal homepage: www.elsevier.com/locate/pss

Combined experimental and theoretical studies on methane photolysis at 121.6 and 248 nm—implications on a program of laboratory simulations of Titan's atmosphere

C. Romanzin, E. Arzoumanian, Et. Es-sebbar, A. Jolly, S. Perrier, M.-C. Gazeau *, Y. Bénilan

LISA, Laboratoire Interuniversitaire des Systèmes Atmosphériques, UMR 7583, Universités Paris 7 et Paris 12, 61 Avenue du Général de Gaulle, 94010 Créteil Cedex, France

ARTICLE INFO

Keywords:
Methane
UV photolysis
Titan
Hydrocarbons
Photochemical model
Experimental simulations

ABSTRACT

Methane is, together with N_2, the main precursor of Titan's atmospheric chemistry. In our laboratory, we are currently developing a program of laboratory simulations of Titan's atmosphere, where methane is intended to be dissociated by multiphotonic photolysis at 248 nm. A preliminary study has shown that multiphotonic absorption of methane at 248 nm is efficient and leads to the production of hydrocarbons such as C_2H_2 (Romanzin et al., 2008). Yet, at this wavelength, little is known about the branching ratios of the hydrocarbon radicals (CH_3, CH_2 and CH) and their following photochemistry. This paper thus aims at investigating methane photochemistry at 248 nm by comparing the chemical evolution observed after irradiation of CH_4 at 248 and at 121.6 nm (Ly-α). It is indeed important to see if the chemistry is driven the same way at both wavelengths in particular because, on Titan, methane photolysis mainly involves Ly-α photons. An approach combining experiments and theoretical analysis by means of a specifically adapted 0-D model has thus been developed and is presented in this paper. The results obtained clearly indicate that the chemistry is different depending on the wavelength. They also suggest that at 248 nm, methane dissociation is in competition with ionisation, which could occur through a three-photon absorption process. As a consequence, 248 nm photolysis appears to be unsuitable to study methane neutral photochemistry alone. The implications of this result on our laboratory simulation program and new experimental developments are discussed. Additional information on methane photochemistry at 121.6 nm are also obtained.

1. Introduction

Titan, the largest moon of Saturn, has a dense atmosphere mainly composed of molecular nitrogen and methane. The dissociation of these two compounds by solar ultraviolet (UV) photons and energetic electrons coming from the magnetosphere of Saturn initiates complex chemical reactions, which lead to the formation of many organic compounds such as nitriles and hydrocarbons. The Cassini–Huygens mission has given the opportunity to achieve a better knowledge of Titan's atmosphere and surface. The data obtained in situ from the Huygens probe as well as those provided by the Cassini spacecraft have revealed some new facets of Titan's atmospheric system. The chemical composition of the upper atmosphere of Titan has been derived from the measurements of an ion neutral mass spectrometer (INMS) instrument on board Cassini orbiter. The data delivered by this instrument have allowed the determination of ethane and hydrogen volume mixing ratios in the upper atmosphere and of the abundances of some carbon–nitrile compounds (C_2H_2, C_2H_4, C_2H_6 and C_3H_4 as well as C_3H_8, C_4H_2, HCN, HC_3N, C_6H_8 and C_2N_2) in the 1230–1174 km altitude range (Waite et al., 2005). As a matter of fact, most of these species have already been identified and quantified earlier in the lower atmosphere, thanks to Cassini Infrared Spectrometer (CIRS) measurements (Flasar et al., 2005). INMS data have also revealed the unexpected presence of heavy and complex molecules at higher altitudes than predicted (above 1200 km) (Vuitton et al., 2006b; Waite et al., 2007).

This new image of Titan's atmospheric chemistry has been further improved by coupling observational results and theoretical modelling (Lavvas et al., 2008a, b). In parallel, some laboratory studies, focusing for instance on the determination of spectroscopic parameters (Bénilan et al., 2006; Jolly et al., 2007; Ferradaz et al., 2009), have allowed the identification of new species in the atmosphere of the satellite. One of the remaining challenges in the understanding of Titan's atmospheric system is to provide a full description of the chemical processes responsible for its evolution. This is the aim of S.E.T.U.P. (a French acronym for Theoretical and Experimental Studies Useful for Planetology), a program of representative simulations based on a unique

* Corresponding author. Tel.: +33 1 45171560
E-mail addresses: claire.romanzin@upmc.fr (C. Romanzin), marie-claire.gazeau@lisa.u-pec.fr (M.-C. Gazeau).

0032-0633/$ - see front matter © 2010 Elsevier Ltd. All rights reserved.
doi:10.1016/j.pss.2010.07.001

experimental device. This new device consists of a reactor where the initial gas mixture will be exposed, for the first time, to both of the major energy sources responsible for the chemical evolution of Titan's atmosphere (i.e. electrons and photons) (Romanzin et al., 2008). Chemistry of nitrogen and photochemistry of methane will thus be combined. So far, in such experiments, the analysis was only performed on the resulting gas sample. From now on, time resolved analysis of intermediates species as well as primary products will be carried out in order to identify the chemical mechanisms taking place in the reactor.

In Titan's atmosphere, photolysis of methane mainly involves Lyman-α photons (121.6 nm ⇔ 10.2 eV). Classical H_2 photochemical lamps can deliver such UV photons. Unfortunately, these continuous sources are not suitable for high-speed kinetic studies. Therefore, in our simulation experiments, the use of a pulsed laser (KrF excimer delivering photons at 248 nm ⇔ 5 eV) has also been considered to photodissociate methane. A comparative methane photolysis study at 121.6 and 248 nm—involving one or two photons respectively—has thus been performed as a first step of our S.E.T.U.P. simulation program. Preliminary results based on IR analysis of the stable products formed after irradiation of CH_4 at both wavelengths have shown that photolysis at 121.6 and 248 nm could be considered as energetically equivalent (two-photon process at 248 nm) (Romanzin et al., 2008). However, the nature and the abundance of the resulting hydrocarbons suggested that the photodissociation channels might be different. To explore this hypothesis, an approach combining similar irradiation experiments and photochemical modelling has been developped and is reported here. This methodology is indeed well suited to test for the accurate description of the different mechanisms involved as already shown by our group in several studies (Smith et al., 1999; Smith and Raulin, 1999; Vuitton et al., 2006a).

The first aim of the present work is to characterize methane photolysis at 248 and 121.6 nm. As discussed in a previous publication, the available literature provides contradictory values for photolytic decomposition pathways at Lyman-α while no data are available at 248 nm (see Romanzin et al., 2005 and references therein). The present study also aims at evaluating the influence of irradiation wavelength on nature and abundance of the resulting photoproducts. In Section 2, we describe two series of methane photolysis experiments performed at 121.6 and 248 nm. Modelling of these experiments is also discussed together with some theoretical aspects of methane photodissociation at both wavelengths. In the third section, the experimental and theoretical results obtained are presented. They are compared and discussed in terms of photolytic decomposition pathways and chemical mechanisms in Section 4. We finally conclude on the implications of this work for the future simulation experiments of Titan's atmosphere within the S.E.T.U.P. program.

2. Experimental and theoretical tools

2.1. Experimental tools

2.1.1. Analytical cell

Irradiations are performed in a 3 L ($V = 3042 \pm 5$ cm^3) stainless steel multireflexion White-cell (Fig. 2) filled with pure methane (CH_4 N45 from Air Liquide) at various pressures depending on the experiments (see Tables 2 and 3). Note that the photolysis cell is pumped down to 10^{-7} mbar prior to new experiment to prevent any contamination. The chemical evolution of the gas mixture resulting from methane irradiation is monitored by a Fourier transform infrared spectrometer (Bruker Equinox 55) operating in the 400–4000 cm^{-1} range. All the spectra were recorded with a spectral resolution of 0.5 cm^{-1} and an optical path length of 500 cm.

2.1.2. Spectroscopic modelling

Infrared spectra are integrated over 15 min (50 scans) during the irradiations to observe the disappearance of methane and the appearance and evolution of the photochemical products (see Fig. 1). Table 1 gives for each observed molecule the center and the integrated strength of bands used to estimate the absolute densities. These are obtained by direct comparison between experimental and synthetic spectra. Calculated spectra have been obtained using line by line spectroscopic parameters from the GEISA database (Jacquinet-Husson et al., 2005). For methane, the comparison was made in the low absorption part of the spectra avoiding strongly saturated zones. In the case of high density acetylene spectra, the strong central Q-branch was also avoided in the comparison. For ethane and ethylene, the molecular densities could be obtained by comparing the complete bands since no saturation was observed.

The detection is not easy for every compound. The ν_5 bending mode of C_2H_2 benefits from a strong integrated band intensity and also from a very strong central Q-branch, which can be observed at very low densities. The ν_7 band of C_2H_4 benefits also from strong band intensity but the central Q-branch is not as sharp as

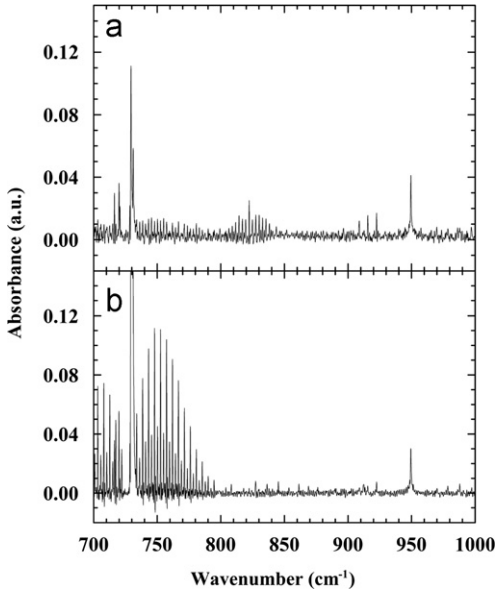

Fig. 1. Absorption infrared spectra of (a) the gaseous mixture after 5.5 h of irradiation at 121.6 nm (see Table 2—experiment 1d for more details) and (b) the gaseous mixture after 15 h of irradiation at 248 nm (see Table 3—experiment 2bE2 for more details).

Table 1
Spectroscopic data.

	Band	$\tilde{\nu}$(cm^{-1})	S_ν [cm^{-2} atm^{-1} at 296 K]	Vibration mode	Reference
C_2H_2	ν_5	729.1	735.0	CH bending	GEISA
C_2H_4	ν_7	949.2	312.8	CH_2 wagging	GEISA
C_2H_6	ν_{12}	822.0	25	CH_3 s-rocking	GEISA
CH_4	ν_3	3019.5	276	CH stretch	GEISA

Please cite this article as: Romanzin, C., et al., Combined experimental and theoretical studies on methane photolysis at 121.6 and 248 nm—implications on a program of laboratory simulations of Titan's atmosphere. Planet. Space Sci. (2010), doi:10.1016/j.pss.2010.07.001

for acetylene. Consequently, the detection limit for ethylene is 8 times higher than for acetylene. The ν_{12} band of C_2H_6 is the most unfavourable case among the three studied photochemical products since it has much lower band intensity and also much dispersed spectra, lacking the strong central feature. As a result, using this band, ethane has a detection limit 25 times higher than for ethylene and thus 200 times higher than acetylene. Assuming a noise level of 2.5×10^{-3} in our absorbance spectra, density limits of 5×10^{11}, 4×10^{12} and 1×10^{14} cm^{-3}, respectively, for C_2H_2, C_2H_4 and C_2H_6 can be inferred from our synthetic spectra calculations. The intense ν_7 band of C_2H_6 around 3000 cm^{-1}could have been used but unfortunately it is superimposed on the CH_4 band and its spectroscopic parameters are poorly known.

2.1.3. CH_4 irradiations at 121.6 nm and actinometry

A schematic drawing of the experimental device used for our Ly-α photolysis experiments is presented in Fig. 2. The cell is equipped with a MgF_2 window (Ø=2.0 cm) allowing the transmission of UV photons delivered by a photochemical discharge flow lamp directly connected to the cell. The gas mixture flowing through the lamp (2% of H_2 in He (quality 4.9) from Linde gas) is excited by a microwave generator (Somelec, France) with a power of 200 W at 2450 MHz. With such a gas mixture, we expect mainly Ly-α photons to be emitted (Brehm and Siegert, 1965). Yet, the emission around 160 nm commonly observed with these kinds of lamps may remain important (Fuchs et al., 1995; Cottin et al., 2003) though this contribution is poorly characterised.

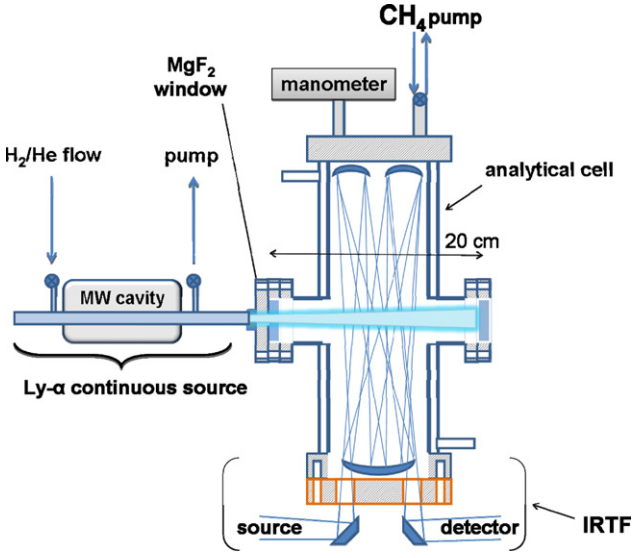

Fig. 2. Schematic drawing of the experimental device used to study methane dissociation at 121.6 nm. Ly-α photons are obtained by exciting an H_2/He gas mixture flowing through the lamp placed in a microwave cavity.

Table 2
Experimental conditions of methane irradiation experiments at Ly-α.

Name	P_{CH4} (atm)	f_0 (10^{15} hν.s^{-1})	Total irradiation time (h)
1a	3.17×10^{-4}	4.4 ± 0.1	25
1b	5.17×10^{-4}	6.4 ± 0.2	7
1c	7.25×10^{-4}	6.8 ± 0.2	5
1d	8.50×10^{-4}	7.0 ± 0.2	6

The photon flux delivered by the lamp has been measured using actinometry (Cottin et al., 2000, and references therein) for each irradiation experiment (Table 2). The photon flux is derived from the CO production rate arising from CO_2 (99.99% from Linde gas) VUV photolysis and has been assumed to be exclusively due to Ly-α photons. The total number of Ly-α photons entering the cell per second, $f_{121.6}$, is then related to the CO production rate through

$$f_{121.6}=\frac{\Delta P_{CO}}{\Delta t}\frac{V}{k_B T}\frac{1}{\phi_{diss,CO_2}.\beta_{CO_2}} \quad (1)$$

where P_{CO} is the CO partial pressure in the cell (Pa), t the time (s), V the volume of the analytical cell (m^3), k_B the Boltzmann constant, T the temperature (K), ϕ_{diss,CO_2} the quantum yield of CO production from CO_2 photolysis at 121.6 nm (here assumed to be equal to unity) and β_{CO_2} the fraction of the flux absorbed by the actinometer CO_2 and determined from the Beer-Lambert law

$$\beta_{CO_2}=1-\frac{I}{I_0}=1-\exp\left[-\varepsilon_{CO_2}^{(121.6)} l P_{CO_2}\right] \quad (2)$$

here $\varepsilon_{CO_2}^{(121.6)}=1.61$ atm^{-1} cm^{-1} (Yoshino et al., 1996), is the absorption cross-section of CO_2 at 121.6 nm, l=22 cm the length of the analytical cell and $P_{CO_2}=5.26\times10^{-3}$ atm the pressure of CO_2 in the analytical cell in our experiments.

A typical actinometry measurement is presented in Fig. 3. The pressure of CO formed after CO_2 irradiation is determined from the integration of the CO band at 2143.2 cm^{-1}. Using the integrated band strength $S_\nu=243.3$ cm^{-2} atm^{-1} from the GEISA database (Jacquinet-Husson et al., 2005), $\Delta P_{CO}/\Delta t$ is retrieved, leading to the determination of $f_{121.6}$ using Eq. (1).

It is nevertheless important to keep in mind that this value does not correspond to the real Ly-α photons flux but to an upper limit. CO_2 photolysis may indeed also occur at 160 nm given the spectral characteristics of the lamp and the absorption cross-section of CO_2 at 160 nm (Yoshino et al., 1996). However, in a first approximation, these extra photons will not be considered here because there is no real quantitative agreement on their contribution to the emission of these kinds of lamps (Brehm and Siegert, 1965; Fuchs et al., 1995; Cottin et al., 2003) in the literature. The lamp flux determined before (referenced as f_0 in Table 2) and after each irradiation experiment shows a mean decrease of maximum 15% per hour attributed to the deposition of solid products on the MgF_2 window. This variation is assumed to be linear with time and has been taken into account in the modelling part of the study (see Section 2.2).

Four irradiations of methane (1a, 1b, 1c and 1d as referenced in Table 2) have been performed at Ly-α. In the analytical cell, CH_4 pressures varying from 3.17×10^{-4} to 8.50×10^{-4} atm have been used. Knowing that the value of the methane extinction coefficient at Ly-α is $\varepsilon_{CH_4}^{(121.6)}=440$ atm^{-1} cm^{-1} (Chen and Wu, 2004), it can be easily determined that 90% of the flux is absorbed at a distance from the MgF_2 window equal to $l\approx13.3$ cm for experiment 1a and $l\approx4.5$ cm for experiment 1d. This means that the chemical mechanisms are initiated much closer to the wall in the second case. The volume where the photolysis takes place (V_{irr}) has been also determined taking into account the divergence of the light beam and is about 47 cm^3 in the first case (1a) and 4 cm^3 in the second case (1d).

The leak rate of the experimental cell has been estimated by following the increase in CO contamination during long-term experiments and is assumed to be negligible ($\sim10^{-3}$ mbar h^{-1}).

2.1.4. CH_4 irradiations at 248 nm

Four photolysis experiments of methane have been performed at 248 nm in the same cell as the one described above (see Fig. 3). Here methane pressures during experiments were 0.148 or

Please cite this article as: Romanzin, C., et al., Combined experimental and theoretical studies on methane photolysis at 121.6 and 248 nm—implications on a program of laboratory simulations of Titan's atmosphere. Planet. Space Sci. (2010), doi:10.1016/j.pss.2010.07.001

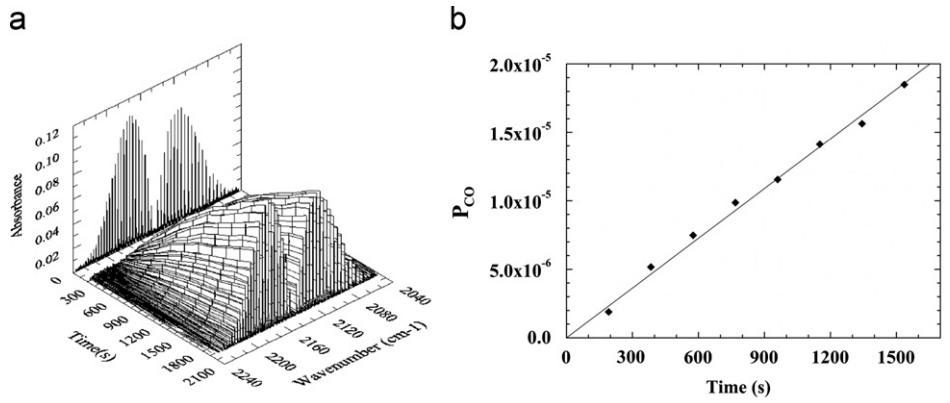

Fig. 3. Determination of the H_2/He lamp flux (121.6 nm) by actinometry—CO appearance in the photolysis cell is directly monitored during irradiation of CO_2. Panel (a) presents the evolution of the CO signature at 2143.2 cm^{-1} as a function of time. The lamp flux is then retrieved from the P_{CO}=f(t) slope shown in panel (b). P_{CO} is in atm.

Table 3
Experimental conditions of methane irradiation experiments at 248 nm.

Name	P_{CH_4} (atm)	E_{laser} (mJ)	Total pulsed irradiation time (h)
2aE1	0.148	80	6.5
2aE2	0.148	120	11
2bE1	0.494	65	7
2bE2	0.494	120	34

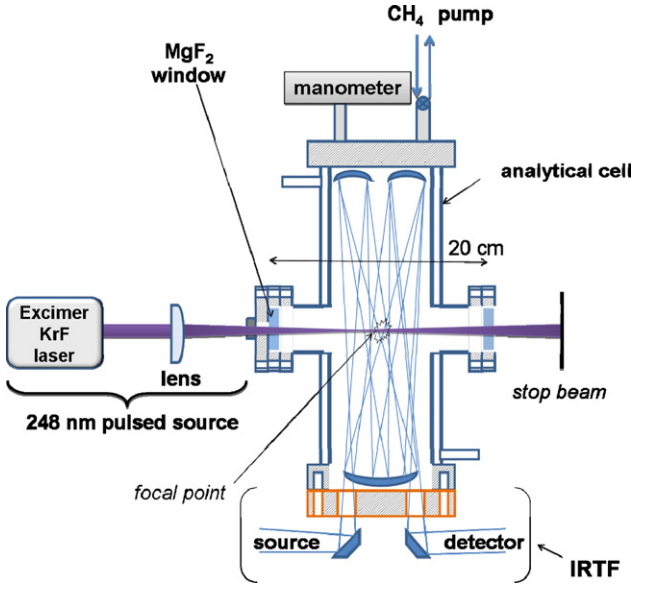

Fig. 4. Schematic drawing of the experimental device used to study methane dissociation at 248 nm. The 248 nm photons are delivered by a KrF excimer laser. A spherical lens (f=19 cm) is used to focus the beam into the cell in order to induce methane mutiphotonic absorption.

0.494 atm (Table 3) and a KrF excimer pulsed laser (Excistar M20, TUI Laser) operating at 10 Hz was used to provide photons at 248 nm as shown in Fig. 4.

The energy delivered within the 20 ns-duration pulse has been varied from 65 to 120 mJ (Joulemeter Gentec, ED-500) corresponding to a photon flux ranging from 4.1 to 7.5×10^{24} $h\nu\ s^{-1}$. Note that the incident laser beam (original size: 15×7 mm^2) is focused into the center of the photolysis cell by means of a spherical lens (f=19 cm) in order to concentrate the laser energy

Table 4
Comparison of the main characteristics of the two UV light sources used in our experiments.

	121.6 nm	248 nm
Photon energy (eV)	10.2	5
Light source	H_2/He lamp	KrF excimer laser
Type of irradiation	continuous	Pulsed (ν=10 Hz, Δt=20 ns)
Photons flux f ($h\nu\ s^{-1}$)	6.2×10^{15} on average	$4.1–7.5 \times 10^{24}$ within a pulse
Beam dimensions	2.0 cm diameter	From 0.7×1.5 cm^2 to 0.6×1 mm^2 (original size–focal point)

in a minimal volume and favour the multiphotonic absorption probability of CH_4. At 248 nm, methane photolysis can indeed proceed only via a multiphotonic absorption process, requiring a high photon fluency F. The mutiphotonic absorption probability $W_{i,n}$ is related to F through

$$W_{i,n} = \sigma_n F^n \quad (3)$$

where σ_n is the cross-section for an n-photons process ($cm^{2n}\ s^{n-1}$) and F the photon fluency ($h\nu\ cm^{-2}\ s^{-1}$). With the laser energies used in our experiments, two-photon absorption processes are expected to dominate (Romanzin et al., 2008). The effective volume where photolysis takes place is thus directly related to the dimensions of the laser beam (Table 4). The size of the laser spot at the center of the cell (focal point) is estimated to be 0.6 mm^2.

2.1.5. Compared characteristics of the two light sources

As described previously, the only difference between the two sets of experiments lies in the nature of the light source. Table 4 gives a comparison of the main characteristics of both types of irradiation we used. Note that it is important to consider the effective irradiation time for laser photolysis if one wants to compare it to the continuous irradiation time with the lamp (see Section 2.2 for details).

2.2. Theoretical tools

A zero-dimension (0-D) photochemical model has been used to predict the chemical evolution of the irradiated gaseous mixture in our experiments. This model is based on a chemical scheme

Please cite this article as: Romanzin, C., et al., Combined experimental and theoretical studies on methane photolysis at 121.6 and 248 nm—implications on a program of laboratory simulations of Titan's atmosphere. Planet. Space Sci. (2010), doi:10.1016/j.pss.2010.07.001

adapted from models previously developed for more complex theoretical studies of Titan's atmosphere (Smith and Raulin, 1999; Hébrard et al., 2005, 2006; Vuitton et al., 2006a; Hébrard et al., 2007). Yet, only the hydrocarbon chemistry part is considered here, leading to a reduced chemical scheme made up of 283 reactions involving 29 neutral species (molecules and radicals containing up to four carbon atoms, see Hébrard et al. (2006) for details of the reactions). The set of differential equations arising from this chemical scheme is then solved using FacSimile software (v.3.0.41 for Windows—Curtis, 1979).

In the model, the chemistry is explicitly detailed and photolysis is described by a photolysis rate directly related to the photolysis constant J (s^{-1}) through Eq. (2):

$$\frac{dC_i}{dt} = -J_i C_i \tag{4}$$

The expression of J has been adapted in order to deal satisfactorily with the experiments described above (see Section 2.1). Indeed, in the experiments, photons are not distributed all over the cell but only within the volume defined by the geometry of the light beam and the effective length of absorption over the cell (see Section 2.1.3). This volume corresponds to the irradiated volume V_{irr} and photolysis does only occur in this region on a limited number of molecules. A correction factor corresponding to the ratio of the irradiated volume over the total volume of the cell V_{irr}/V_{tot} is thus applied to J. The different nature of the two photolytic processes implied in our experiments has also been taken into account by adapting the expression of J with respect to the nature of the light source considered. It results in the following expressions:

(i) at 121.6 nm

$$J_i^{121.6} = \frac{V_{irr}}{V_{tot}} \phi_{diss,i} \sigma_i F_0 \tag{5}$$

where V_{irr} is the volume of the region where photolysis occurs (cm^3), V_{tot} the total volume of the cell (cm^3), $\phi_{diss,i}$, the dissociation quantum yield of the molecule i, σ_i the absorption cross-section of the molecule i (cm^2)and F_0 the incident photon flux ($h\nu\ cm^{-2}\ s^{-1}$)

(ii) at 248 nm

$$J_i^{248} = \frac{V_{irr}}{V_{tot}} \phi_{diss,i} \langle W_{i,2} \rangle \tag{6}$$

where $\langle W_{i,2} \rangle$ is the average value of the two-photon absorption probability for i. V_{irr} the volume of the region where photolysis occurs (cm^3) and V_{tot} the total volume of the cell (cm^3).

$\langle W_{i,2} \rangle$ is estimated on the basis of the laser photolysis fluency averaged over the beam path into the experimental cell. We indeed assume that in our experimental conditions the 248 nm methane photolysis corresponds to a two-photon process according to our previous results (Romanzin et al., 2008). The two-photon absorption cross-section σ_2 has been taken equal to $2.7 \times 10^{-53}\ cm^4\ s\ photon^{-1}$ as estimated by Galasso (1992) from theoretical calculations.

This photolysis description has been applied to methane and to C_2 hydrocarbons for the modelling of the 121.6 nm irradiation experiments but only to methane for the 248 nm ones. Indeed, secondary photolysis of the hydrocarbons resulting from the chemistry induced by methane photolysis at 248 nm has been assumed to be negligible. The weak absorption cross-section of these compounds at 248 nm (see Table 5 for detailed references) precludes the single-photon photolysis process and the probability of a two-photon photolysis process is assumed to be really small according to the low density of these molecules with respect to methane. Table 5 summarizes the different sets of branching ratios which have been used in our model. For methane, the scheme of Wang et al. (2000) has been applied because this scheme is based on a whole set of experimental data and thus appears to be the most reliable one to date.

Other parameters have also been adapted to account for the specificities of the two light sources. This is especially the case for the laser pulsed irradiation experiments, where the photon flux f delivered within a pulse has been scaled down by a factor $\nu\,\Delta t = 2 \times 10^{-7}$ in order to obtain an effective continuous photon flux of easier use in the model. It indeed allows considerable reduction of the computing time and simulation of the evolution of the gaseous mixture over a longer period without introducing any significant bias in the simulation outputs as shown in Fig. 5.

Table 5
Photolysis schemes of CH_4, C_2H_2, C_2H_4 and C_2H_6 at 10.2 eV used in our 121.6 nm model. For the 248 nm model, only methane photolysis has been considered and as no data are available at this wavelength, the set of branching ratios of CH_4 at 121.6 nm has been used in a first approximation. References for both branching ratios and absorption cross-sections are specified in the table.

Dissociation channels		Φ	References	
$CH_4 + h\nu \rightarrow$	$CH_3 + H$	(a)	0.291	Φ: (Wang et al., 2000)
	$^1CH_2 + H_2$	(b)	0.585	σ_{abs}: (Vatsa and Volpp, 2001)
	$^3CH_2 + 2H$	(c)	0.000	
	$^1CH_2 + 2H$	(d)	0.066	
	$CH + H + H_2$	(e)	0.068	
$C_2H_2 + h\nu \rightarrow$	$C_2H + H$	(a)	0.30	Φ: (Okabe, 1981, 1983; Seki and Okabe, 1993),
	$C_2 + H_2$	(b)	0.10	σ_{abs}: (Nakayama and Watanabe, 1964; Vattulainen et al., 1997; Bénilan et al., 2000)
$C_2H_4 + h\nu \rightarrow$	$C_2H_2 + H_2$	(a)	0.58	Φ: (Holland et al., 1997; Chang et al., 1998)
	$C_2H_2 + 2H$	(b)	0.42	σ_{abs}: (Zelikoff and Watanabe, 1953; Orkin et al., 1997)
$C_2H_6 + h\nu \rightarrow$	$C_2H_4 + H_2$	(a)	0.12	Φ: (Akimoto et al., 1965; Hampson and McNesby, 1965a, 1965b; Lias et al., 1970)
	$C_2H_4 + 2H$	(b)	0.30	σ_{abs}: (Lee et al., 2001)
	$C_2H_2 + H + H_2$	(c)	0.25	
	$CH_4 + {}^1H_2CH_3 + CH_3$	(d)	0.25	
		(e)	0.08	

Please cite this article as: Romanzin, C., et al., Combined experimental and theoretical studies on methane photolysis at 121.6 and 248 nm—implications on a program of laboratory simulations of Titan's atmosphere. Planet. Space Sci. (2010), doi:10.1016/j.pss.2010.07.001

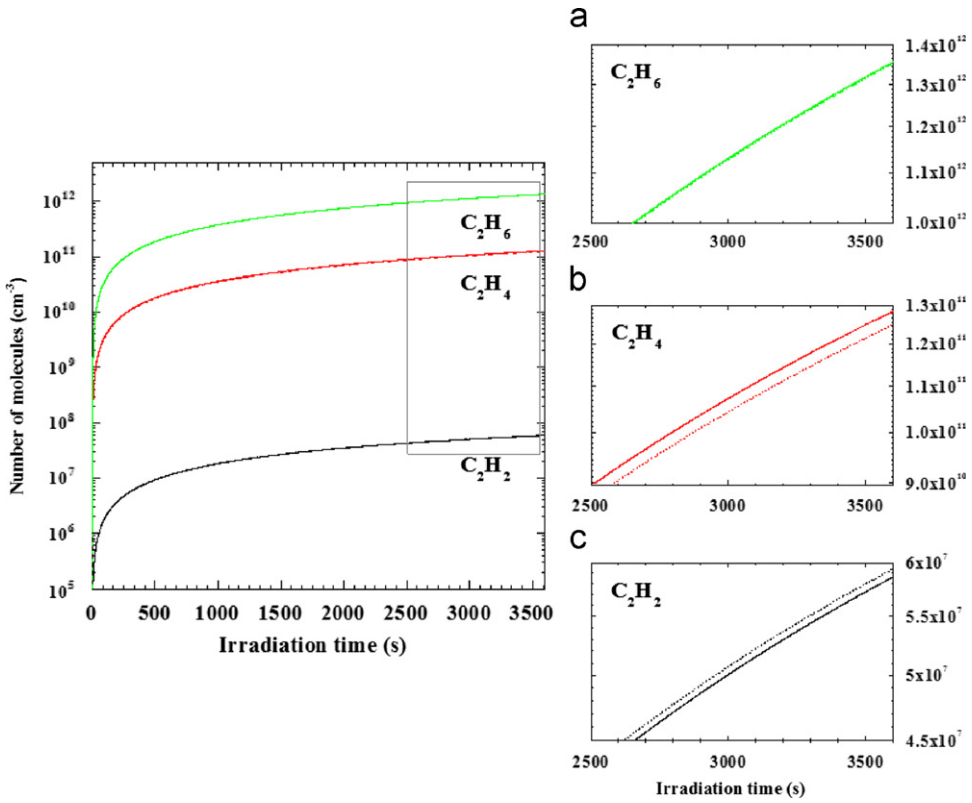

Fig. 5. Density profiles of the main resulting hydrocarbons after 1 h of irradiation according to a test model where 248 nm photolysis is described as continuous (straight lines) or pulsed (dashed lines).

The photochemical model described here has been applied to the modelling of both types of methane photolysis experiments. The evolution of chemical complexity within the gaseous mixture can thus be followed through the computed concentration profiles as a function of time. The different results obtained will be discussed with respect to the experimental ones in Section 3.

3. Results

3.1. Methane Ly-α photolysis

3.1.1. Experimental results at Ly-α

Fig. 6 presents the concentration profiles as a function of time of the main products observed – C_2H_2, C_2H_4 and C_2H_6 – for three Ly-α irradiations: 1b–1d corresponding to CH_4 initial pressures of 5.17×10^{-4}, 7.25×10^{-4} and 8.50×10^{-4} atm, respectively. The global evolution observed for the three products is the same—after a first increase, the density reaches a plateau between 2 and 5 h of irradiation. In each case, C_2H_6 is the major product and C_2H_4 reaches rapidly its maximum whereas C_2H_2 evolves slower but reaches higher density at longer time scales. These different behaviours lead to a crossing of the two density profiles as a function of time. This crossing seems to be related to the initial pressure of methane and occurs earlier as methane initial concentration increases. This remarkable point will help to constrain the photochemical modelling of the experiments and will be discussed in more detail in the following section.

3.1.2. Modelling of Ly-α photolysis experiments

The 0-D photochemical model described in Section 2.2 has been used to simulate experiments 1a–1d and infer some information on the photochemical evolution of the gaseous mixtures. The model outputs follow the same global behaviour for all experiments. Here we will focus our discussion on experiments 1a and 1d corresponding, respectively, to a long irradiation and a "high-pressure" experiment (see Table 2). The corresponding results are presented in Fig. 7. From this figure, it appears that the use-up of methane is overestimated by the model as well as ethane production especially during the first 5–6 h of irradiation. On the other hand, ethylene and acetylene are slightly underestimated at the very beginning of the experiment. Yet, relative concentrations of the products and general trends are satisfactorily reproduced. Crossing between the density profiles is also predicted though better agreement is obtained for low-pressure experiment (1a). However, the long-term behaviour of the different density profiles (left panel) is not perfectly reproduced since no important decrease is observed unlike what is predicted by the model.

The overestimation of methane photolytic destruction can be explained by considering the photon flux delivered by the lamp. The estimated photon flux is indeed overestimated because the fraction of light absorbed by CO_2 and responsible for CO formation is assumed to be exclusively due to Ly-α photons though lower energy photons are also delivered by the lamp (see Section 2.1.3) and absorbed by CO_2 (Yoshino et al., 1996). The real fraction of photons absorbed by CO_2, β_{CO_2}, is thus larger than estimated. As a result, the real photon flux is lower than the one presented in Table 2 and also includes the contribution of wavelengths different from Ly-α (mainly 160 nm). The photolysis constants J for all the compounds are thus overestimated in the model, especially for CH_4 and C_2H_6, which do not absorb at 160 nm. This is consistent with the enhanced destruction rate of methane predicted by the model. It could also explain the pronounced decrease in the model outputs for C_2H_2, C_2H_4 and C_2H_6 after 10 h (left panel). Yet, this will not play in favour of a rapid growth of

Please cite this article as: Romanzin, C., et al., Combined experimental and theoretical studies on methane photolysis at 121.6 and 248 nm—implications on a program of laboratory simulations of Titan's atmosphere. Planet. Space Sci. (2010), doi:10.1016/j.pss.2010.07.001

C_2H_2 and C_2H_4 concentration profiles at the beginning of the experiments. So some further investigations on the spectral characteristics of these lamps have to be done if one wants to be able to disentangle the different photochemical processes and identify the key processes. Kinetic uncertainties may also be responsible for some of the discrepancies observed (Hébrard et al., 2007). A specific study should be performed but at ambient temperature these uncertainties should be less critical.

3.2. 248 nm photolysis of CH_4

Results of methane irradiation experiments at 248 nm are presented in Fig. 8. The only products observed are C_2H_2 and C_2H_4,

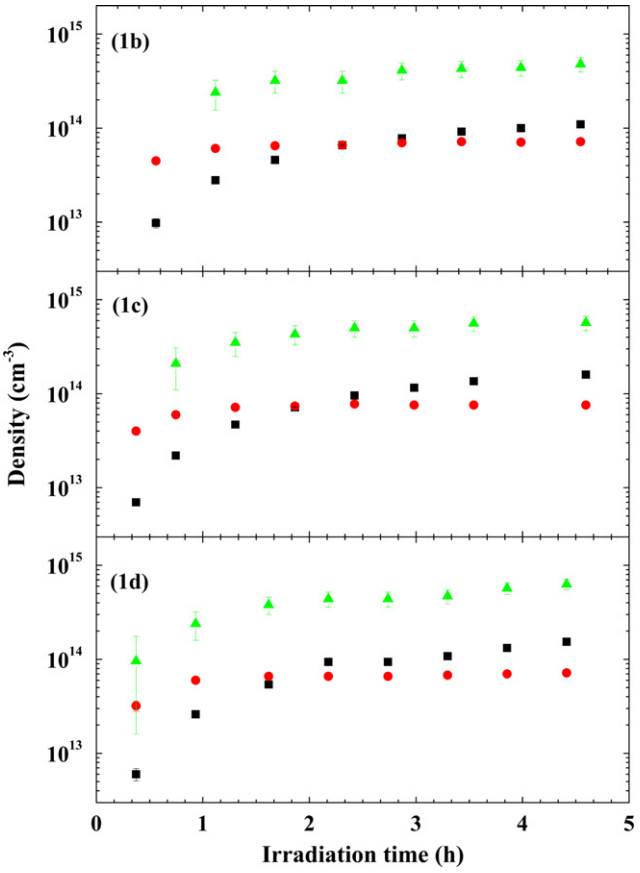

Fig. 6. Evolution of the densities of C_2H_2 (black squares), C_2H_4 (red circles) and C_2H_6 (green triangles) as a function of time for Ly-α irradiation experiments 1b (top), 1c (middle) and 1d (bottom) as referenced in Table 2. (For interpretation of the references to color in this figure legend, the reader is referred to the web version of this article.)

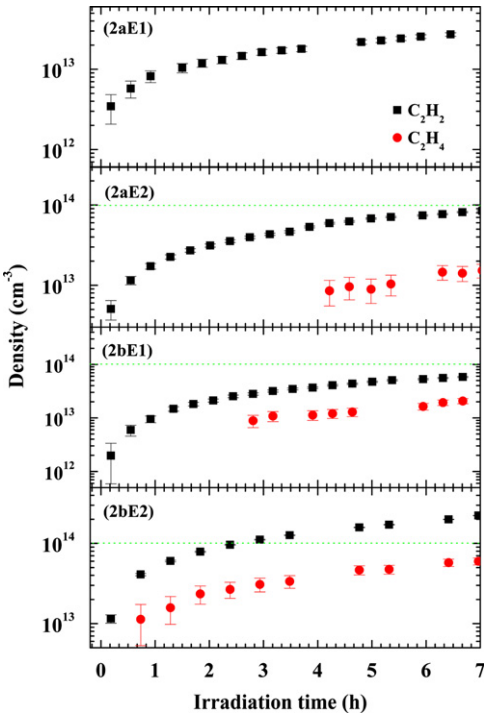

Fig. 8. Evolution of the densities of C_2H_2 (black squares) and C_2H_4 (red circles) as a function of time for 248 nm irradiation experiments as referenced in Table 2. The green dotted line corresponds to the limit of detection of C_2H_6. (For interpretation of the references to color in this figure legend, the reader is referred to the web version of this article.)

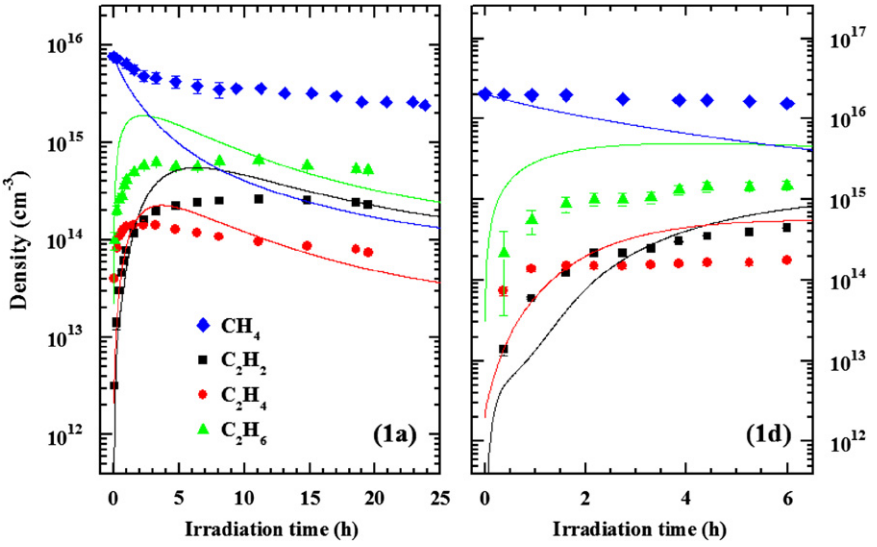

Fig. 7. Compared evolution of the simulated and experimental concentration profiles for experiments 1a (left column) and 1d (right column).

Please cite this article as: Romanzin, C., et al., Combined experimental and theoretical studies on methane photolysis at 121.6 and 248 nm—implications on a program of laboratory simulations of Titan's atmosphere. Planet. Space Sci. (2010), doi:10.1016/j.pss.2010.07.001

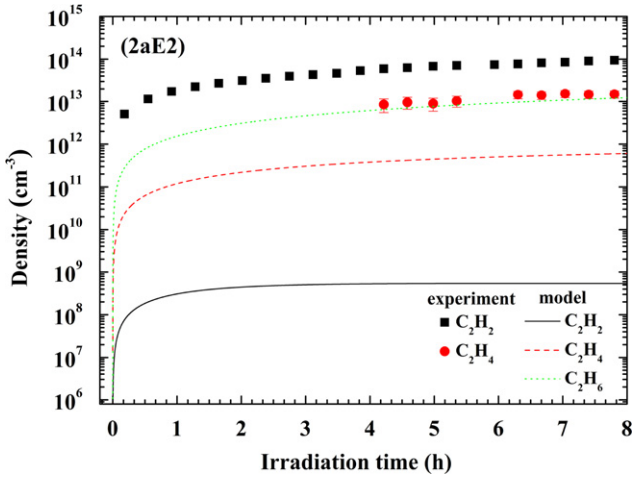

Fig. 9. Compared evolution of the densities of C_2H_2 (black squares) and C_2H_4 (red circles) as a function of time for 248 nm irradiation experiment 2aE2 with respect to the model ouputs for C_2H_2 (black solid line), C_2H_4 (red dashed line) and C_2H_6 (green dotted line). (For interpretation of the references to color in this figure legend, the reader is referred to the web version of this article.)

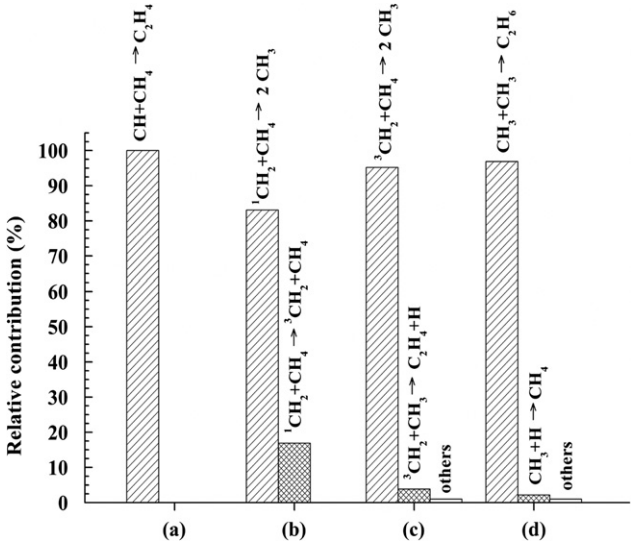

Fig. 10. Main contributions to the destruction of (a) CH, (b) $^1CH_2$, (c) $^3CH_2$ and (d) CH_3 according to the model after 4 h of photolysis at 248 nm in the conditions of experiment 2bE1.

C_2H_2 being the most abundant in all cases. However, the most striking result here is the absence of ethane (in the limit of our detection sensitivity that is 1×10^{14} cm^{-3} for C_2H_6) among the final products even after 34 h of irradiation (experiment (2bE2)) whereas C_2H_6 was the major photolysis product at 121.6 nm and that comparable amounts of C_2H_2 are observed at both wavelengths. Different assumptions have thus been considered in order to explain this unexpected behaviour.

First of all, if we assume a two-photon absorption, as expected from our previous study, we should take into account the possibility that at 248 nm, the branching ratios may be different from the ones assumed at 121.6 nm. This hypothesis has been tested by exploring different sets of branching ratios for CH_4 in the model described in Section 2.2. Yet, none of them could account for the experimental observations (see Fig. 9). In fact, the model outputs exhibit little dependence when methane branching ratios are varied—C_2H_6 is always expected to be the main product of methane photolysis although it is almost exclusively formed by association of two methyl radicals with the following reaction:

$$CH_3+CH_3+M\rightarrow C_2H_6 \quad (7)$$

This can be understood if the evolution of the photofragments is carefully considered. Analysis of the model outputs thus reveals that 90% of the CH_3 radicals react to form C_2H_6. So, as expected, any significant changes in the ethane concentration profile are observed when increasing the weight of channel (a). The same behaviour is observed if more weight is given to channels (b)–(d), leading to $^{1,3}CH_2$. From Fig. 10, it indeed appears that both species are very efficiently converted to CH_3 by collisions with the surrounding CH_4. If you besides consider the evolution of the CH_3 radicals, the absence of ethane in the resulting gaseous mixture cannot be explained. Let us now consider channel (e) leading to CH. As can be seen from Fig. 10, it almost exclusively reacts with CH_4 to give C_2H_4, so one might expect the balance between the model products to be more in favour of C_2H_4 than of C_2H_6. However, ethane is once again the main product to be formed according to the model and the discrepancy stays large because ethylene further efficiently reacts with H atoms to form C_2H_5, which in turn is converted to two CH_3 radicals by reaction with H and these methyl radicals mainly lead to the formation of an ethane molecule. So other processes have to be considered to account for experimental observations at 248 nm.

If we go on with the assumptions made in the 248 nm model, we may also question the absence of secondary photolysis. It could indeed account for the non-detection of C_2H_6 in our experiments. However when secondary photolysis of the main hydrocarbons (i.e. C_2H_2, C_2H_4 and C_2H_6) is taken into account, C_2H_6 remains the major photolysis product according to the model.

It is for instance also possible that, given the high laser fluence used in our experiments (see Section 2.1.4), methane absorbs more than two photons. The energy deposited would then be higher than the ionisation threshold of methane (with $PI_{CH_4}=12.61$ eV, (Hunter and Lias, 2009)) and the presence of CH_4^+ ions in the gaseous mixture could be responsible for the observed chemical evolution. Ion-neutral chemistry is indeed not described in our model. Moreover, some electronic excited states of CH_4 are accessible in the 10 eV region (Heck et al., 1996; Mebel et al., 1997) and can act as relay states for a third photon absorption. This third absorption step would thus be resonant and much more efficient than the first two absorption steps, leading to an apparent multiphotonic order of two though three photons are effectively absorbed. This could be an explanation for the results obtained in our previous study (Romanzin et al., 2008).

4. Conclusions

A comparative study of methane photolysis at 121.6 and 248 nm has been performed in order to estimate to what extent the photolysis wavelength could affect the nature and the abundance of the resulting photochemical products. This is of importance for our new simulation program of Titan's atmosphere (S.E.T.U.P.), in which methane photolysis is intended to be performed by means of a pulsed laser delivering 248 nm photons. The experimental results obtained when comparing the products observed after photolysis of methane at 121.6 and 248 nm using, respectively, a photochemical lamp and a KrF laser show that the chemical evolution following methane photolysis is significantly different depending on the wavelength: at 121.6 nm, ethane is the principal product formed whereas at 248 nm it is not observed

Please cite this article as: Romanzin, C., et al., Combined experimental and theoretical studies on methane photolysis at 121.6 and 248 nm—implications on a program of laboratory simulations of Titan's atmosphere. Planet. Space Sci. (2010), doi:10.1016/j.pss.2010.07.001

and C_2H_2 is mainly produced. The analysis of these experiments by means of a 0-D photochemical model suggests that methane photolysis at 248 nm most likely also involves the absorption of three photons rather than only two as expected. Thus, in addition to photodissociation, methane is also probably photoionized at 248 nm. New chemical reaction networks including ion/neutral reaction chemistry, must be considered to account for the presence of ionic species in the gaseous mixture and reproduce the observed concentration profiles.

These results clearly indicate that multiphotonic photolysis at 248 nm is not suitable to study pure neutral chemistry initiated by CH_4 photolysis; a VUV pulsed source must be developed to achieve the primary goal of the S.E.T.U.P. program, that is to provide a full description of the chemical processes through time resolved analysis of the system. These developments will be carried out in the near future but in the meantime a photochemical lamp will be used to photodissociate CH_4. As discussed in the introduction, this will not allow us to probe the reactive intermediates and no information could be retrieved on fast kinetic processes. Yet it will still be possible to study the kinetic evolution of the stable products. Nevertheless, according to the results from the present study, some further experiments to better define and constrain the flux delivered by the lamp are necessary to improve our understanding of the photochemical mechanisms driving the evolution of the gaseous mixture. This will be of primary importance for the future experiments where CH_4 photolysis and N_2 dissociation by means of energetic electrons, that have been independently characterised (Es-sebbar et al., 2009), will be coupled.

Acknowledgements

The authors wish to acknowledge the CNRS (PNP grant), the CNES, the "Région Ile de France" and University Paris 12 for financial support. C.R. would like to acknowledge Dr. É. Hébrard and Dr. M. Camredon for their great help in the development of the photochemical model.

References

Akimoto, H., Obi, K., Tanaka, I., 1965. Primary process in the photolysis of ethane at 1236 Å. The Journal of Chemical Physics 42 (11), 3864–3868.

Bénilan, Y., Smith, N., Jolly, A., Raulin, F., 2000. The long wavelength range temperature variations of the mid-UV acetylene absorption coefficient. Planetary and Space Science 48 (5), 463–471.

Bénilan, Y., Jolly, A., Raulin, F., Guillemin, J.-C., 2006. IR band intensities of DC_3N and HC_3N^{15}: implication for observations of Titan's atmosphere. Planetary and Space Science 54 (6), 635–640.

Brehm, v.B., Siegert, H., 1965. Eine intensive H_2-entladungslampe für das ferne vakuum ultraviolett. Zetschrift für Angewandte Physik 3, 244–246.

Chang, A., Mebel, A., Yang, X., Lin, S., Lee, Y., 1998. Ab initio/RRKM approach toward the understanding of ethylene photodissociation. Journal of Chemical Physics 109 (7), 2748–2761.

Chen, F.Z., Wu, C.Y.R., 2004. Temperature-dependent photoabsorption cross sections in the VUV–UV region. I. Methane and ethane. Journal of Quantitative Spectroscopy and Radiative Transfer 85, 195–209.

Cottin, H., Gazeau, M.-C., Doussin, J.-F., Raulin, F., 2000. An experimental study of the photodegradation of polyoxymethylene at 122, 147 and 193 nm. Journal of Photochemistry and Photobiology A: Chemistry 135, 53–64.

Cottin, H., Moore, M.H., Bénilan, Y., 2003. Photodestruction of relevant interstellar molecules in ice mixtures. The Astrophysical Journal 590, 874–881.

Curtis, 1979. Facsimile.

Es-sebbar, E., Bénilan, Y., Jolly, A., Gazeau, M.-C., 2009. Characterization of an N_2 flowing microwave post-discharge by OES spectroscopy and determination of absolute ground-state nitrogen atom densities by TALIF. Journal of Physics D: Applied. Physics 42, 135206.

Ferradaz, T., Bénilan, Y., Fray, N., Jolly, A., Schwell, M., Gazeau, M.-C., Jochims, H.W., 2009. Temperature-dependant photoabsorption cross-sections of cyanoacetylene and diacetylene in the mid- and vacuum-UV: application to Titan's atmosphere. Planetary and Space Science 57 (1), 10–22.

Flasar, F.M., Achterberg, R.K., Conrath, B.J., Gierasch, P.J., Kunde, V.G., Nixon, C.A., Bjoraker, G.L., Jennings, D.E., Romani, P.N., Simon-Miller, A.A., Bézard, B., Coustenis, R.C., Irwin, P.G.J., Teanby, N.A., Brasunas, J., Pearl, J.C., Segura, M.E., Carlson, R.C., Mamoutkine, A., Schinder, P.J., Barucci, A., Courtin, R., Fouchet, T., Gautier, D., Lellouch, E., Marten, A., Prangé, R., Vinatier, S., Strobel, D.F., Calcutt, S.B., Read, P.L., Taylor, F.W., Bowles, N., Samuelson, R.E., Orton, G.S., Spilker, L.J., Owen, T.C., Spencer, J.R., Showalter, M.R., Ferrari, C., Abbas, M.M., Raulin, F., Edgington, S., Ade, P., Wishnow, E.H., 2005. Titan's atmospheric temperatures, winds, and composition. Science 308 (975-978).

Fuchs, C., Goetzberger, O., Henck, R., Fogarassy, E., 1995. Polymer photoablation under windowless VUV hydrogen or helium discharge lamp. Applied Physics A 60, 505–507.

Galasso, V., 1992. Ab initio study of mutiphoton absorption properties of methane, ethane, propane, and butane. Chemical Physics 161, 189–197.

Hampson, R.F., McNesby, J.R., 1965a. Vacuum-ultraviolet photolysis of ethane at high temperature. The Journal of Chemical Physics 42 (6), 2200–2208.

Hampson, R.F., McNesby, J.R., 1965b. Vacuum-ultraviolet photolysis of ethane at high temperature. II. Collisional deactivation of excited ethylene. The Journal of Chemical Physics 43 (10), 3592–3596.

Hébrard, E., Benilan, Y., Raulin, F., 2005. Sensitivity effects of photochemical parameters uncertainties on hydrocarbon production in the atmosphere of Titan. Advances in Space Research 36 (2), 268–273.

Hébrard, E., Dobrijevic, M., Bénilan, Y., Raulin, F., 2006. Photochemical kinetics uncertainties in modeling Titan's atmosphere: a review. Journal of Photochemistry and Photobiology C: Photochemitry Reviews 7 (4), 211–230.

Hébrard, E., Dobrijevic, M., Bénilan, Y., Raulin, F., 2007. Chemical kinetics uncertainties in modeling Titan's atmosphere. Planetary and Space Science 55 (10), 1470–1489.

Heck, A.J.R., Zare, R.N., Chandler, D.W., 1996. Photofragment imaging of methane. Journal of Chemical Physics 104 (11), 4019–4030.

Holland, D., Shaw, D., Hayes, M., Shpinkova, L., Rennie, E., Karlsson, L., Baltzer, P., Wannberg, B., 1997. A photoabsorption, photodissociation and photoelectron spectroscopy study of C_2H_4 and C_2D_4. Chemical Physics 219 (1), 91–116.

Hunter, E.P., Lias, S.G., 2009. Gas phase ion energetics data. In: WebBook de Chimie NIST, Base de Données Standard de référence NIST.

Jacquinet-Husson, N., Scott, N.A., Chédin, A., Garceran, K., Armante, R., Chursin, A.A., Barbe, A., Birk, M., Brown, L.R., Camy-Peyret, C., Claveau, C., Clerbaux, C., Coheur, P.F., Dana, V., Daumont, L., Debacker-Barilly, M.R., Flaud, J.M., Goldman, A., Hamdouni, A., Hess, M., Jacquemart, D., Köpke, P., Mandin, J.Y., Massie, S., Mikhailenko, S., Nemtchinov, V., Nikitin, A., Newnham, D., Perrin, A., Perevalov, V.I., Régalia-Jarlot, L., Rublev, A., Schreier, F., Schult, I., Smith, K.M., Tashkun, S.A., Teffo, J.L., Toth, R.A., Tyuterev, V.G., Auwera, J.V., Varanasi, P., Wagner, G., 2005. The 2003 edition of the GEISA/IASI spectroscopic database. Journal of Quantitative Spectroscopy and Radiative Transfer 95 (4), 429–467.

Jolly, A., Bénilan, Y., Fayt, A., 2007. New infrared integrated band intensities for HC_3N and extensive line list for the ν_5 and ν_6 bending modes. Journal of Molecular Spectroscopy 242 (1), 46–54.

Lavvas, P.P., Coustenis, A., Vardavas, I.M., 2008a. Coupling photochemistry with haze formation in Titan's atmosphere, part I: model description. Planetary and Space Science 56 (1), 27–66.

Lavvas, P.P., Coustenis, A., Vardavas, I.M., 2008b. Coupling photochemistry with haze formation in Titan's atmosphere, part II: results and validation with Cassini/Huygens data. Planetary and Space Science 56 (1), 67–99.

Lee, A., Yung, Y., Cheng, B., Bahou, M., Chung, C., Lee, Y., 2001. Enhancement of deuterated ethane on Jupiter. The Astrophysical Journal 551 (1), L93–L96.

Lias, S.G., Collin, G.J., Rebbert, R.E., Ausloos, P., 1970. Photolysis of Ethane at 11.6–11.8 eV. The Journal of Chemical Physics 52 (4), 1841–1851.

Mebel, A.M., Lin, S.-H., Chang, C.-H., 1997. Theoretical study of vibronic spectra and photodissociation pathways of methane. Journal of Chemical Physics 106 (7), 2612–2620.

Nakayama, T., Watanabe, K., 1964. Absorption and photoionisation coefficients of acetylene, propyne and 1-butyne. Journal of Chemical Physics 40 (2), 558–561.

Okabe, H., 1981. Photochemistry of acetylene at 1470 Å. The Journal of Chemical Physics 75 (6), 2772–2778.

Okabe, H., 1983. Photochemistry of acetylene at 1849 Å. Journal of Chemical Physics 78 (3), 1312–1317.

Orkin, V., Huie, R., Kurylo, J., 1997. Rate constants for the reactions of OH with HFC-245cb.

Romanzin, C., Gazeau, M.-C., Benilan, Y., Hebrard, E., Jolly, A., Raulin, F., Boyé-Peronne, S., Douin, S., Gauyacq, D., 2005. Methane photochemistry: a brief review in the frame of a new experimental program of Titan's atmosphere simulations. Advances in Space Research 36 (2), 258–267.

Romanzin, C., Bénilan, Y., Jolly, A., Gazeau, M.-C., 2008. Photolytic behaviour of methane at Lyman-α and 248 nm: studies in the frame of a simulation program of Titan's atmosphere (S.E.T.U.P.). Advances in Space Research 42 (12), 2036–2044.

Seki, K., Okabe, H., 1993. Photochemistry of acetylene at 193.3 nm. Journal of Physical Chemistry 97 (20), 5284–5290.

Smith, N., Gazeau, M.-C., Khelifi, A., Raulin, F., 1999. A combined experimental and theoretical study of the catalytic dissociation of methane by the photolysis of acetylene at 185 nm. Planetary and Space Science 47, 3–10.

Smith, N.S., Raulin, F., 1999. A box model of the photolysis of methane at 123.6 nm and 147 nm-comparison between model and experiment. Journal of Photochemistry and Photobiology A: Chemistry 124, 101–112.

Vatsa, R.K., Volpp, H.R., 2001. Absorption cross-sections for some atmospherically important molecules at the H atom Lyman-α wavelength (121.567 nm). Chemical Physics Letters 340, 289–295.

Please cite this article as: Romanzin, C., et al., Combined experimental and theoretical studies on methane photolysis at 121.6 and 248 nm—implications on a program of laboratory simulations of Titan's atmosphere. Planet. Space Sci. (2010), doi:10.1016/j.pss.2010.07.001

Vattulainen, J., Wallenius, L., Stenberg, J., Hernberg, R., Linna, V., 1997. Experimental determination of SO_2, C_2H_2 and O_2 absorption cross sections at elevated temperatures and pressures. Applied Spectroscopy 57, 1311–1315.

Vuitton, V., Doussin, J.-F., Bénilan, Y., Raulin, F., Gazeau, M.-C., 2006a. Experimental and theoretical study of hydrocarbon photochemistry applied to Titan stratosphere. Icarus 185 (1), 287–300.

Vuitton, V., Yelle, R.V., Anicich, V.G., 2006b. The nitrogen chemistry of Titan's upper atmosphere revealed. The Astrophysical Journal Letters 647 (2), L175–L178.

Waite Jr., J.H., Niemann, H., Yelle, R.V., Kasprzak, W.T., Cravens, T.E., Luhmann, J.G., McNutt, R.L., Ip, W.-H., Gell, D., de La Haye, V., Muller-Wordag, I., Magee, B., Borggren, N., Ledvina, S., Fletcher, G., Walter, E., Miller, R., Scherer, S., Thorpe, R., Xu, J., Block, B., Arnett, K., 2005. Ion neutral mass spectrometer results from the first flyby of Titan. Science 308 (5'724), 982–986.

Waite Jr., J.H., Young, D.T., Cravens, T.E., Coates, A.J., Crary, F.J., Magee, B., Westlake, J., 2007. The process of tholin formation in Titan's upper atmosphere. Science 316 (5826), 870–875.

Wang, J.-H., Liu, K., Min, Z., Su, H., Bersohn, R., Preses, J., Larese, J.Z., 2000. Vacuum ultraviolet photochemistry of CH_4 and isotopomers. II. Product channel fields and absorption spectra. Journal of Chemical Physics 113 (10), 4146–4152.

Yoshino, K., Esmond, J.R., Sun, Y., Parkinson, W.H., Ito, K., Matsui, T., 1996. Absorption cross-section measurements of carbon dioxide in the wavelength region 118.7–175.5 nm and the temerature dependance. Journal of Quantitative Spectroscopy and Radiative Transfer 55 (1), 53–60.

Zelikoff, M., Watanabe, K., 1953. Absorption coefficient of ethylene in the vacuum ultraviolet. Journal of the American Optical Society 43 (9), 756–759.

Please cite this article as: Romanzin, C., et al., Combined experimental and theoretical studies on methane photolysis at 121.6 and 248 nm—implications on a program of laboratory simulations of Titan's atmosphere. Planet. Space Sci. (2010), doi:10.1016/j.pss.2010.07.001